Taylor & Francis
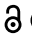Taylor & Francis Group

RESEARCH PAPER

OPEN ACCESS   Check for updates

Vitamin D₃ and carbamazepine protect against *Clostridioides difficile* infection in mice by restoring macrophage lysosome acidification

Hung Chan[a,b,c], Qing Li[a,b,c,d], Xiansong Wang[a,b], Wing Yingzhi Liu[a,b], Wei Hu[a,b,c], Judeng Zeng[a,b,c], Chuan Xie[a,b,c], Thomas Ngai Yeung Kwong[c,d,e], Idy Hiu Ting Ho[a,b,c], Xiaodong Liu[a,b,c], Huarong Chen[a,b,c,d], Jun Yu[c,d,e,f], Ho Ko[b,c,e], Raphael Chiu Yeung Chan[g], Margaret Ip [f,g], Tony Gin[a,b,c], Alfred Sze Lok Cheng[d,h], Lin Zhang[a,b,c,d,e], Matthew Tak Vai Chan[a,b,c], Sunny Hei Wong [c,d,e,f,i], and William Ka Kei Wu[a,b,c,d,f]

aDepartment of Anaesthesia and Intensive Care, The Chinese University of Hong Kong, Hong Kong Special Administrative Region, China; bPeter Hung Pain Research Institute, The Chinese University of Hong Kong, Hong Kong Special Administrative Region, China; cLi Ka Shing Institute of Health Sciences, The Chinese University of Hong Kong, Hong Kong Special Administrative Region, China; dState Key Laboratory of Digestive Diseases, The Chinese University of Hong Kong, Hong Kong Special Administrative Region, China; eDepartment of Medicine and Therapeutics, The Chinese University of Hong Kong, Hong Kong Special Administrative Region, China; fCentre for Gut Microbiota Research, The Chinese University of Hong Kong, Hong Kong Special Administrative Region, China; gDepartment of Microbiology, The Chinese University of Hong Kong, Hong Kong Special Administrative Region, China; hSchool of Biomedical Sciences, The Chinese University of Hong Kong, Hong Kong Special Administrative Region, China; iLee Kong Chian School of Medicine, Nanyang Technological University, Singapore

ABSTRACT

Clostridioides difficile infection (CDI) is a common cause of nosocomial diarrhea. TcdB is a major *C. difficile* exotoxin that activates macrophages to promote inflammation and epithelial damage. Lysosome impairment is a known trigger for inflammation. Herein, we hypothesize that TcdB could impair macrophage lysosomal function to mediate inflammation during CDI. Effects of TcdB on lysosomal function and the downstream pro-inflammatory SQSTM1/p62-NFKB (nuclear factor kappa B) signaling were assessed in cultured macrophages and in a murine CDI model. Protective effects of two lysosome activators (i.e., vitamin D₃ and carbamazepine) were assessed. Results showed that TcdB inhibited CTNNB1/β-catenin activity to downregulate MITF (melanocyte inducing transcription factor) and its direct target genes encoding components of lysosomal membrane vacuolar-type ATPase, thereby suppressing lysosome acidification in macrophages. The resulting lysosomal dysfunction then impaired autophagic flux and activated SQSTM1-NFKB signaling to drive the expression of IL1B/IL-1β (interleukin 1 beta), IL8 and CXCL2 (chemokine (C-X-C motif) ligand 2). Restoring MITF function by enforced MITF expression or restoring lysosome acidification with 1α,25-dihydroxyvitamin D₃ or carbamazepine suppressed pro-inflammatory cytokine expression *in vitro*. In mice, gavage with TcdB-hyperproducing *C. difficile* or injection of TcdB into ligated colon segments caused prominent MITF downregulation in macrophages. Vitamin D₃ and carbamazepine lessened TcdB-induced lysosomal dysfunction, inflammation and histological damage. In conclusion, TcdB inhibits the CTNNB1-MITF axis to suppress lysosome acidification and activates the downstream SQSTM1-NFKB signaling in macrophages during CDI. Vitamin D₃ and carbamazepine protect against CDI by restoring MITF expression and lysosomal function in mice.

Abbreviations: ATP6V0B: ATPase H+ transporting V0 subunit b; ATP6V0C: ATPase H+ transporting V0 subunit c; ATP6V0E1: ATPase H+ transporting V0 subunit e1; ATP6V1H: ATPase H+ transporting V1 subunit H; CBZ: carbamazepine; CDI: *C. difficile* infection; CXCL: chemokine C-X-X motif ligand; IL: interleukin; LAMP1: lysosomal-associated membrane protein 1; LC3: microtubule-associated protein 1 light chain 3; LEF: lymphoid enhancer binding factor 1; MITF: melanocyte inducing transcription factor; NFKB: nuclear factor kappa B; PMA: phorbol 12-myristate 13-acetate; TcdA: Clostridial toxin A; TcdB: Clostridial toxin B; TFE3: transcription factor E3; TFEB: transcription factor EB.

Introduction

Clostridioides difficile infection (CDI) is the most common infectious cause of diarrhea among the elderly admitted to the hospitals or in long-term care facilities, and it inflicts a large burden on the health care system [1–3]. CDI typically occurs after the use of antibiotics owing to the disruption of the normal gut microbiota, allowing for the overgrowth of *C. difficile*. Toxin A (TcdA) and toxin B (TcdB) are major

exotoxins secreted by *C. difficile* and they play a key role in the pathogenesis of CDI by inducing macrophage activation, pro-inflammatory cytokine release, neutrophil infiltration, and epithelial cell damage [4–6]. An inflammatory cascade is responsible for many aspects of the pathology associated with *C. difficile*-associated diarrhea [7].

Macrophages are a major source of pro-inflammatory cytokines that contribute to neutrophil recruitment during CDI

[8,9]. Emerging studies have elucidated the specific mechanisms by which TcdA and TcdB stimulate the pro-inflammatory cytokine release from macrophages. Both TcdA and TcdB could activate NLRP3 (NLR family pyrin domain containing 3) inflammasomes to induce IL1B/IL-1β (interleukin 1 beta) secretion in macrophages and human mucosal biopsy specimens [10]. TcdB could also activate CASP1 (caspase 1) via pyrin inflammasomes [11]. Functionally, genetic ablation of PYCARD/ASC (PYD and CARD domain containing), a key component of all subtypes of inflammasomes, dampened toxin-induced inflammation and damage [10]. Aside from the inflammasome pathway, activation of NFKB (nuclear factor kappa B) signaling in macrophages is implicated in the cytokine response during CDI [12]. Nevertheless, the upstream machinery underlying *C. difficile*-triggered NFKB activation is currently unclear. In this regard, inhibition of WNT-CTNNB1/β-catenin signaling due to the binding of TcdB to the frizzled proteins has been described as an upstream event in the pathogenesis of CDI [13]. Since exaggerated inflammation is associated with worse outcome in CDI patients [14,15], modulating the host pro-inflammatory response is a potential therapeutic approach against CDI.

MITF (melanocyte inducing transcription factor) is a transcription factor which belongs to the basic helix-loop-helix leucine zipper family. It is a master regulator of macroautophagy/autophagy and lysosomal biogenesis by translocating into the nucleus to stimulate expression of genes important for lysosomal structure and function, including vacuolar-type ATPase pumps and lysosomal enzymes such as acid ceramidase [16–18]. Because lysosomal dysfunction is known to exacerbate inflammation and tissue damage in different inflammatory and autoimmune disorders [15], we postulated that deregulation of lysosomes and the upstream regulator(s) are involved in CDI pathogenesis. Here, we show the blocking effect of TcdB on the WNT-CTNNB1/β-catenin signaling to suppress MITF transcriptional activity to reduce vacuolar ATPase gene expression, thereby promoting lysosomal dysfunction and autophagic flux impairment in macrophages during CDI. This action triggered SQSTM1/p62 accumulation and activated NFKB to induce the expression of pro-inflammatory cytokines.

Results

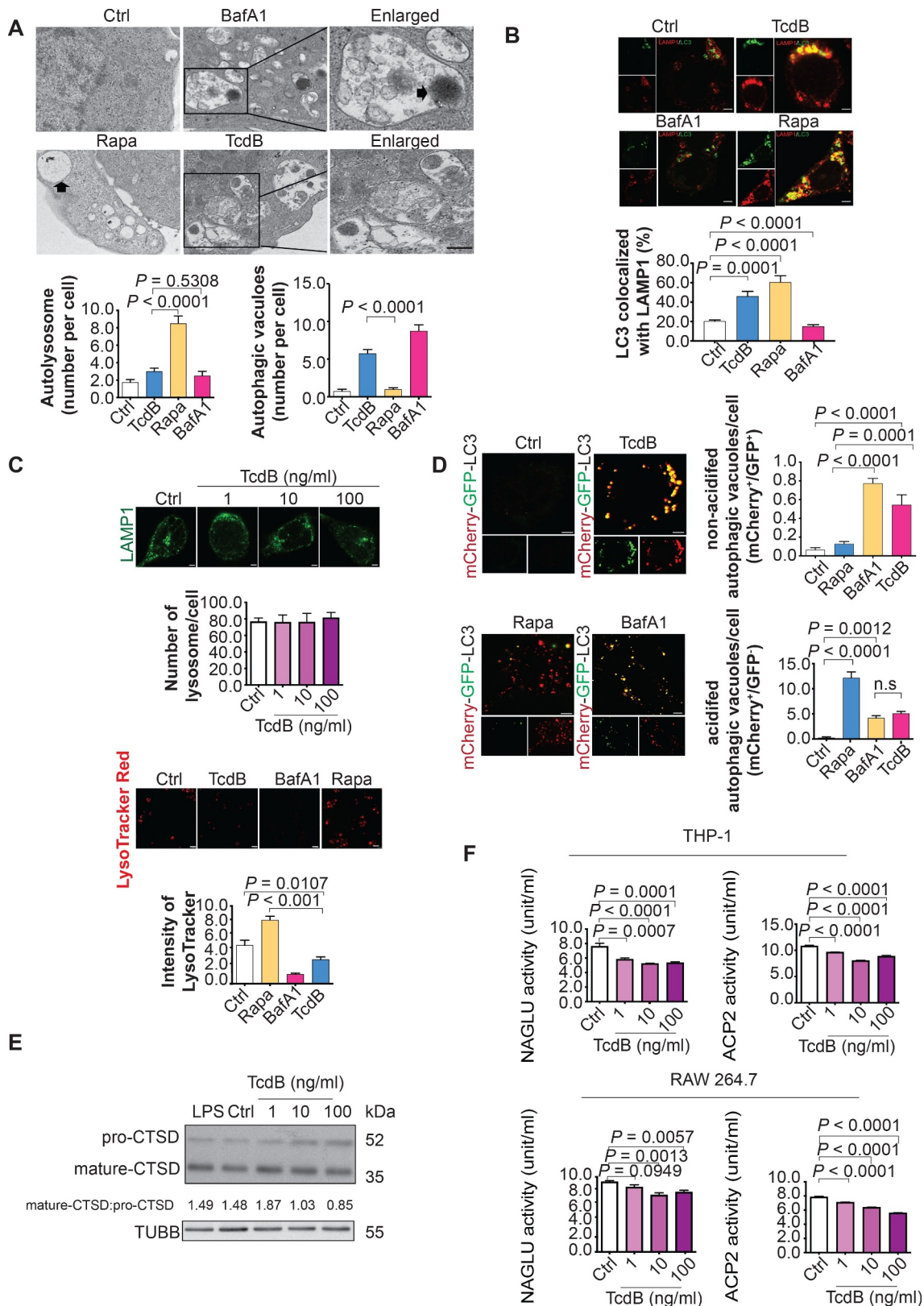### TcdB induced pro-inflammatory cytokines through SQSTM1/p62-dependent NFKB activation in macrophages

We first measured mRNA levels of three pro-inflammatory cytokines relevant to CDI [19,20], namely *IL1B, IL8* and *CXLC2*, which were induced upon exposure of the macrophages to various concentrations of TcdB (Figure 1B). The induction was peaked at 6 h (Figure 1A and Fig. S1A). TcdB enhanced the mRNA expression of all three pro-inflammatory cytokines in a concentration-dependent manner (Figure 1 and Fig. S1B). Since the canonical NFKB pathway is a major intracellular pathway mediating the induction of pro-inflammatory genes in macrophages [21], we further determined whether the pro-inflammatory response triggered by

TcdB was associated with NFKB activation. We observed that TcdB decreased the levels of total NFKBIA/IKB (an inhibitor of NFKB), enhanced the phosphorylation of NFKB RELA/p65 subunit at serine 536, and increased RELA/p65 nuclear translocation (Figure 1C and Fig. S1C). To determine the mechanism by which TcdB activated NFKB, we examined the role of autophagy since SQSTM1/p62 (an autophagic receptor accumulated during autophagic flux impairment) is a well-established upstream activator of NFKB [22,23]. Consistent with our hypothesis, TcdB induced the concomitant accumulation of LC3-II and SQSTM1/p62 (left panel of Figure 1D and Fig. S1D), which is suggestive of autophagic flux impairment [24]. Additionally, a combination of TcdB and bafilomycin A_1 induced no further increase in SQSTM1/p62 protein levels when compared with cells treated with bafilomycin A_1 alone (right panel of Figure 1D). These data demonstrated that TcdB impaired autophagic flux by inhibiting the clearance of autophagosomes. Importantly, knockdown of SQSTM1/p62 abolished TcdB-induced NFKB RELA/p65 phosphorylation (Figure 1E and Fig. S1E) as well as *IL1B, IL8* and *CXCL2* mRNA expression (Figure 1F and Fig. S1F), confirming the role of impaired autophagic flux in NFKB activation in TcdB-exposed macrophages.

TcdB impaired autophagic flux by suppressing lysosome acidification in macrophages

Since Western blot results indicated that TcdB might impede the autophagic flux (Figure 1D and Fig. S1D), we examined if TcdB could induce accumulation of non-digestive autophagosomes in macrophages by TEM (transmission electron microscopy). Quantitative analysis of TEM images revealed an increased number of double-membrane structures containing undigested organelles and aggregates, consistent with the accumulation of non-digestive autophagosomes upon impaired autophagic flux, in TcdB-exposed macrophages (Figure 2A). We further determined if hindered autophagosome–lysosome fusion or reduced lysosome-dependent degradation was responsible for the observed autophagic flux impedance by TcdB. By visualizing colocalization of GFP-MAP1LC3/LC3 (microtubule associated protein 1 light chain 3; an autophagosome marker) with LAMP1 (lysosomal associated membrane protein 1; a lysosome marker), we found that TcdB did not affect autophagosome–lysosome fusion (Figure 2B). Instead, TcdB significantly decreased the number of acidic lysosomes without affecting the total of number of lysosomes as revealed by LysoTracker Red staining and immunofluorescence of LAMP1, respectively (Figure 2C). Consistently, THP-1 macrophages transfected with the GFP-mCherry-LC3B plasmid showed a strong retention of GFP fluorescent signal colocalized with mCherry (Figure 2D), suggesting the accumulation of nonacidic autophagosomes [24]. We did not perform the GFP-mCherry-LC3B assay in RAW 264.7 murine macrophages because of the low transfection efficiency. The inhibition of lysosome acidification was also corroborated by the findings that TcdB inhibited the conversion of pro-CTSD (cathepsin D) into mature CTSD (a pH-dependent process; Figure 2E) and reduced the activities of two classical lysosomal enzymes – ACP2 (acid phosphatase 2,

Figure 1. Pro-inflammatory cytokine induction, autophagic flux impairment and NFKB activation by TcdB in human PMA-differentiated THP-1 macrophages. (A) Effects of exposure to TcdB (10 ng/ml) for the indicated time periods on the mRNA levels of *IL1B, IL8* and *CXCL2* in cultured THP-1 macrophages. (B) Effects of exposure to TcdB at the indicated concentrations for 6 h on the mRNA levels of *IL1B, IL8,* and *CXCL2* in cultured THP-1 macrophages. LPS (100 ng/ml) was used as a positive control. (C) Exposing macrophages to TcdB (10 ng/ml) for 6 h decreased the protein levels of NFKBIA/IKB, enhanced NFKB RELA/p65 phosphorylation at serine 536, and promoted the nuclear translocation of NFKB RELA/p65 (green). Cytoplasmic and nuclear localization of NFKB RELA/p65 were visualized by immunofluorescence. Nuclei (blue) were labeled with DAPI. A total of 50 cells from each group were randomly selected for quantification by the ImageJ software. Scale bar: 5 μm (D) Exposing macrophages to TcdB (10 ng/ml) for 6 h led to increased protein levels of both LC3-II and SQSTM1/p62 (left panel). Exposing macrophages to TcdB (10 ng/ml) in the presence of bafilomycin A₁ (200 μM) for 6 h induced no further increase in SQSTM1/p62 protein levels (right panel). (E-F) Knockdown of *SQSTM1* with siRNA abolished TcdB (10 ng/ml; 6 h)-induced (E) NFKB RELA/p65 phosphorylation at serine 536 and (F) mRNA expression of *IL1B, IL8,* and *CXCL2*. Protein and mRNA levels were quantified by Western blots and RT-qPCR, respectively. Results are expressed as mean ± S.E.M. from three independent experiments.

Figure 2. Impairment of autophagic flux and lysosome acidification by TcdB in macrophages. (A) Ultrastructural alterations induced by TcdB (10 ng/ml, 6 h) in PMA-differentiated THP-1 cells were visualized by TEM. The typical images of autolysosomes (arrow) and autophagosomes enclosing intact undigested cargo (arrowhead) are shown at higher magnification. Scale bar: 2 μm (Enlarged; Scale bar: 200 nm) (n = 3 for each treatment; 10 fields for each biological replicate were used for quantification). (B) Autophagosome-lysosome fusion was assessed by measuring the colocalization of LC3-positive autophagosomes with LAMP1-positive lysosomes in PMA-differentiated THP-1 cells. TcdB (10 ng/ml, 6 h) induced autophagosome-lysosome fusion to an extent similar to that of rapamycin (500 nM, 6 h), a drug for inducing autophagy with unimpeded flux. Scale bar: 5 μm (C) TcdB (10 ng/ml, 6 h) reduced the intensity of LysoTracker Red without affecting total lysosome number as stained by immunofluorescence for LAMP1. A total of 50 cells from each group were randomly selected for quantification by the ImageJ software. Scale bar: 5 μm (D) TcdB-induced impairment of lysosome/autolysosome acidification in PMA-differentiated THP-1 cells was confirmed by mCherry-GFP-LC3 assay. Acidified (digestive) and non-acidified (non-digestive) LC3-positive autophagosomes were visualized under a confocal microscope. Bafilomycin A$_1$ (BafA1; 200 μM, 6 h) was used as a control to impair lysosome acidification and autophagic flux. A total of 20 cells from each group were randomly selected for quantification by the ImageJ software. Scale bar: 5 μm (E) Effects of TcdB (6 h) at the indicated concentrations on the proteolytic cleavage of pro-CTSD into the mature form in PMA-differentiated THP-1 cells. LPS did not affect the proteolytic cleavage. Scale bar: 5 μm (F) TcdB (6 h) at the indicated concentrations reduced the activities of two classical lysosomal enzymes – ACP2 and NAGLU in human and murine macrophages. Results are expressed as mean ± S.E.M. from three independent experiments.

lysosomal) and NAGLU/β-N-acetylglucosaminidase, which are known to be active in acidic conditions (Figure 2F) [25–27].

TcdB downregulated lysosomal proton pump subunits through targeting the CTNNB1/β-catenin-MITF axis

Since transcription factors of the MiTF/TFE family are known to control lysosomal function and biogenesis, we examined the expression of its three family members (TFEB [transcription factor EB], MITF, and TFE3 [transcription E3]) in TcdB-exposed macrophages. We found that *MITF* was downregulated by TcdB whereas *TFEB* and *TFE3* remained unchanged at mRNA level (Figure 3A). The downregulation of MITF at protein level was also confirmed (Figure 3A). To assess how TcdB inhibited lysosome acidification, we further examined the mRNA levels of four subunits (*ATP6V0B* [ATPase H+ transporting V0 subunit b], *ATP6V1H* [ATPase H+ transporting V1 subunit H], *ATP6V0E1* [ATPase H + transporting V0 subunit e1] and *ATP6V0C* [ATPase H + transporting V0 subunit c]) of the lysosomal proton pump (also known as vacuolar-type ATPase). Reverse transcription-quantitative PCR (RT-qPCR) showed that TcdB repressed mRNA transcription of all four subunits (Figure 3B). To ascertain the effect of TcdB-induced downregulation of lysosomal proton pump subunits on lysosome acidification, we overexpressed two of the downregulated lysosomal proton pump subunits (*ATP6V1H* and *ATP6V0E1*) in human macrophages. Results demonstrated that overexpressing *ATP6V1H* or *ATP6V0E1* partially rescued TcdB-triggered lysosome neutralization as shown by LysoTracker Red staining (Fig. S2). Chromatin immunoprecipitation (ChIP)-sequencing with anti-MITF antibody to pull down MITF-bound chromatin further demonstrated that TcdB reduced the occupancy of MITF at its downstream genes, including the four lysosomal proton pump subunits, near their transcription start sites (−2000 bp to +2000 bp; Figure 3C). The genes pulled down in the control group were also enriched in biological processes, such as "autophagy" and "melanogenesis" (Figure 3C), which are known biological functions of MITF [13,14]. Since TcdB was reported to block the WNT-CTNNB1 /β-catenin signaling to induce tissue damage [28], we examined if this pathway was involved in MITF downregulation. Western blots and luciferase assays showed that TcdB strongly reduced the levels of active CTNNB1/β-catenin, the nuclear translocation of CTNNB1/β-catenin, as well as the levels of LEF1 (lymphoid enhancer binding factor 1) and TCF7L2 (transcription factor 7 like 2) (Figure 3D). LEF1 and TCF7L2 are binding partners of CTNNB1/β-catenin for WNT-CTNNB1/β-catenin signaling activation. TcdB also downregulated the promoter activity of MITF (Figure 3E). Moreover, a LEF-binding motif was identified in the MITF promoter, in which site-directed mutagenesis of this motif abolished the inhibition of MITF promoter activity by TcdB (Figure 3E). Moreover, overexpressing three different MITF isoforms (*MITF-A, MITF-M, MITF-D*) antagonized TcdB-induced autophagy flux impairment (Figure 3F), downregulation of MITF and its four lysosomal proton pump subunits (Figure 3G), as well as the induction of *IL1B, IL8* and *CXCL2*

(Figure 3H). To consolidate the regulation of MITF and autophagic flux by TcdB, conditioned medium of *C. difficile* clinical isolates with varied ability to secrete TcdB were co-cultured with macrophages. In line with the experiments with recombinant TcdB, *C. difficile* isolates with higher TcdB production were found to trigger more drastic downregulation of *MITF* (Figure 4A) and accumulation of SQSTM1/p62 and LC3-II (Figure 4B).

Aside from regulating cytokine response, lysosomes are essential for clearing phagocytosed microorganisms in macrophages, in which defective lysosomal degradation has been found to reduce the phagocytic activity [29]. Consistently, TcdB-exposed macrophages exhibited reduced viability (Figure 5A) and attenuated abilities to phagocytose *Escherichia coli* (Figure 5B) and fluorescein-labeled dextran (Figure 5C). Consistent with the central role of MITF in maintaining lysosome function, enforced expression of *MITF* abolished TcdB-provoked impairment of phagocytosis in human macrophages (Figure 5D).

Lysosome activators 1α,25-dihydroxyvitamin D₃ and carbamazepine restored autophagic flux and attenuated cytokine response in vitro

Results presented so far suggested that reduced lysosome acidification mediated the pro-inflammatory effect of TcdB in macrophages. Therefore, we tested if two known pharmacological activators of lysosomes, namely 1α,25-dihydroxyvitamin D₃ (the active form of vitamin D₃) and CBZ, could ameliorate TcdB-induced autophagic flux impairment and pro-inflammatory cytokine expression [25,30]. We demonstrated that both 1α,25-dihydroxyvitamin D₃ and CBZ restored the autophagic flux as evidenced by the abolition of TcdB-triggered accumulation of LC3-II and SQSTM1/p62 (Figure 6A and Fig. S3A). The restoration of lysosome acidification was also confirmed by the unimpeded processing of pro-CTSD into mature CTSD (Figure 6A and Fig. S3A). Notably, 1α,25-dihydroxyvitamin D₃ and CBZ rescued the downregulation of *MITF* and the four lysosomal proton pump subunits (Figure 6B and Fig. S3B) and abolished the induction of *IL1B, IL8* and *CXCL2* by TcdB (Figure 6C, D and Fig. S3C, D).

Vitamin D₃ and carbamazepine ameliorated symptoms and attenuated lysosome dysfunction, cytokine response and histological damage in both murine CDI and colon ligation models

We next examined the potential protective effects of vitamin D₃ and CBZ in a murine CDI model (Figure 7A), following challenge with a TcdB-hyperproducing *C. difficile* strain VPI 10463. This TcdB-hyperproducing strain was frequently used in mouse models to study CDI. C57BL/6 male mice infected with 1×10^8 CFU of VPI 10463 developed clinical features of CDI, including lethargy, diarrhea, and mucosal ulceration associated with neutrophil influx [31].We demonstrated that pre-treatment with vitamin D₃ (2300 IU/kg by oral gavage) or CBZ (50 mg/kg by oral gavage) every other day for 2 weeks ameliorated the CDI symptoms (i.e. weight loss and diarrhea;
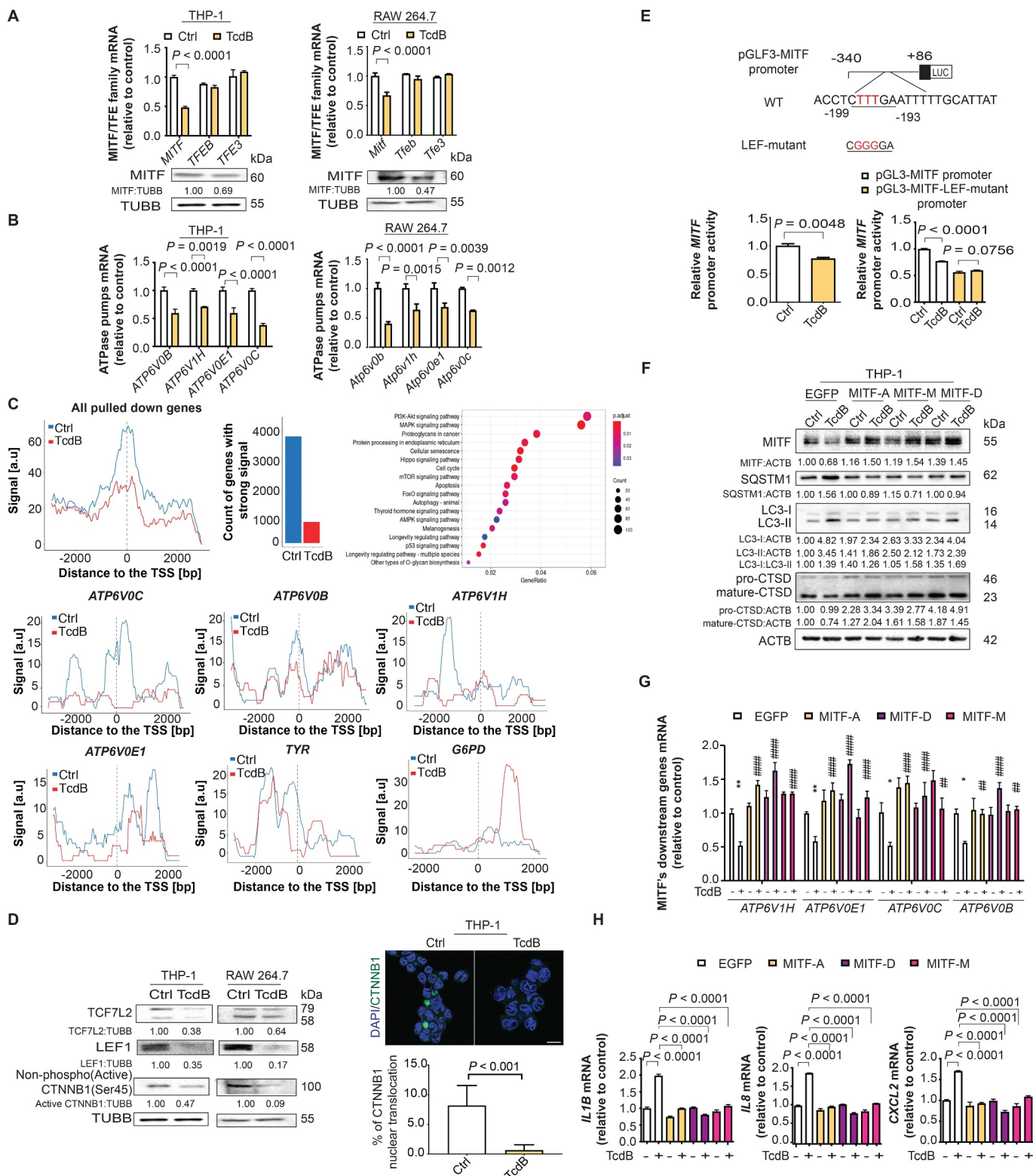
Figure 3. TcdB-mediated pro-inflammatory response through the CTNNB1/β-catenin-LEF-MITF-lysosome proton pump pathway in macrophages. (A) Effects of TcdB (10 ng/ml; 6 h) on mRNA levels of three MITF/TFE family transcriptional factors (*MITF, TFEB, TFE3*) are shown. The downregulation of MITF by TcdB at protein level was confirmed. (B) TcdB (10 ng/ml; 6 h) reduced mRNA levels of the lysosomal proton pump subunits (*ATP6V0C, ATP6V1H, ATP6V0B, ATP6V0E1*). (C) ChIP-sequencing analysis showed that TcdB diminished the occupancy of MITF at regions (−2000 bp to +2000 bp) near the transcription start site (TSS) of the pulled down protein-coding genes in PMA-differentiated THP-1 macrophages. The enrichment of the pulled down genes in biological processes by KEGG analysis is shown. Besides, TcdB diminished the occupancy of MITF near TSS of genes encoding lysosomal proton pump subunits (*ATP6V0C, ATP6V1H, ATP6V0B, ATP6V0E1*). *TYR* and *G6PD* serve as positive and negative control for MITF occupancy, respectively. (D) Effects of TcdB (10 ng/ml; 6 h) on the protein levels of WNT signaling transcription factors (TCF7L2, LEF1 and active CTNNB1/β-catenin) and nuclear translocation of CTNNB1/β-catenin (green) are shown. Cytoplasmic and nuclear localization of CTNNB1/β-catenin were visualized by immunofluorescence. Nuclei (blue) were labeled with DAPI. A total of 50 cells from each group were randomly selected for quantification by the ImageJ software. Scale bar: 20 μm. (E) TcdB reduced the promoter activity of MITF as determined by luciferase assay in PMA-differentiated THP-1 cells. The effects of site-directed mutagenesis of LEF1-binding site on *MITF* promoter activity in the absence or presence of TcdB (10 ng/ml; 6 h) are shown. (F) Effects of TcdB without or with enforced expression of *MITF* isoforms (*MITF-A, MITF-M, MITF-D*) on autophagic flux and proteolytic CTSD processing in PMA-differentiated THP-1 cells are shown.

Cells transfected with EGFP-encoding plasmids were used as a control. (G and H) Effects of TcdB without or with enforced expression of *MITF* isoforms on mRNA levels of (G) lysosomal proton pump subunits and (H) pro-inflammatory cytokines in PMA-differentiated THP-1 cells are shown. Protein and mRNA levels were quantified by Western blots and RT-qPCR, respectively. Results are expressed as mean ± S.E.M. from three independent experiments. *, $p < 0.05$; **, $p < 0.01$; ****, $p < 0.0001$ when compared with the TcdB-unexposed, EGFP-transfected group. ##, $p < 0.01$; ####, $p < 0.0001$ when compared with the TcdB-exposed, EGFP-transfected group.

Figure 7C and 7D for the effects of vitamin D_3; Figure 7G and 7H for the effects of CBZ), the histological damage (i.e. submucosal edema, neutrophilic inflammation and epithelial damage; Figure 7B and 7E for the effects of vitamin D_3; Figure 7F and 7I for the effects of CBZ), as well as the intestinal colonization of *C. difficile* (Fig. S4). To validate the occurrence of *MITF* downregulation and lysosome dysfunction in our murine CDI model, we isolated the macrophages from colonic tissues by cell sorting as illustrated by Figure 8A. In line with our *in-vitro* findings, gavage with a TcdB-hyperproducing *C. difficile* strain downregulated the mRNA expression of *Mitf* and the four lysosomal proton pump subunits (Figure 8B and 8C), suppressed lysosome acidification (Figure 8D), and induced *Il1b, Il8* and *Cxcl2* mRNA expression (Figure 8E and 8F) in colonic macrophages. Pretreatment with vitamin D_3 or CBZ attenuated such alterations (Figure 8B and 8E for the effects of vitamin D_3; Figure 8C and 8F for the effects of CBZ). Similar protective effects of vitamin D_3 and CBZ against CDI were demonstrated in female mice (Fig. S5). To confirm the direct pathogenic involvement of TcdB in lysosome dysfunction during CDI, we applied the colon loop ligation assay as illustrated by Figure 9A and 9B. In line with our TcdB-hyperproducing *C. difficile* strain model, injection of TcdB into sealed colon segments resulted in the same histological damage (Figure 9C). We further isolated the macrophages from TcdB-injected colonic segments, in which TcdB was found to suppress mRNA levels of *MITF* and ATPase pumps accompanied by impairment of lysosome acidification (Figure 9D–9F) and enhanced mRNA expression of pro-inflammatory cytokines (*Il1b, Il8* and *Cxcl2*) in colonic macrophages (Figure 9G). Consistently, pre-treatment with vitamin D_3 or CBZ ameliorated such dysregulation (Figure 9D–9G).

Discussion

TcdA and TcdB are two major exotoxins secreted by *C. difficile* contributing to the pathogenesis of CDI. Both toxins have been reported to engage the pyrin inflammasomes by inactivation of RhoA (Ras homolog gene family member A) GTPase in mouse bone marrow-derived macrophages [32]. We observed that, while both TcdA and TcdB could induce *IL1B, IL8* and *CXCL2* mRNA expression in macrophages, the effects of TcdB were stronger than that of TcdA (Fig. S6). In addition, it is known that TcdA only results in minimal intestinal damage in animal models [33]. Therefore, we focused on TcdB in the present study. We found that TcdB downregulated the CTNNB1/β-catenin-MITF axis to suppress lysosome acidification and thereby inducing the SQSTM1/p62-NFKB signaling to drive the expression of pro-inflammatory cytokines in macrophages during CDI. While

lysosome dysfunction and the resulting autophagic flux impairment have been demonstrated to contribute to different diseases, including Alzheimer disease [34], Parkinson disease [35], nonalcoholic fatty liver diseases [36], intracellular bacterial infections [37,38] and sepsis [39], their role in the pathogenesis of CDI is previously unknown. Herein, we showed that downregulation of MITF, a master control of lysosome function, played a central mechanistic role in the TcdB cascade. In line with our findings, emerging evidence supports that loss of MITF promotes inflammation by increasing chemokine/cytokine expression. For instance, downregulation of MITF could increase JUN/c-Jun expression to amplify TNF/tumor necrosis factor-stimulated cytokine expression in melanoma [40]. Moreover, MITF is downregulated in cardiac tissues during myocardial infarction, in which enforced expression of MITF reduces inflammatory injury [41]. Concordantly, our data support that restoration of MITF expression is key to the therapeutic response to vitamin D_3 and carbamazepine in CDI.

While our data support that lysosome dysfunction in macrophages plays a key role in CDI, it is noteworthy that the effect of TcdB on lysosome function might be cell type-dependent. Here, we showed that exposure to TcdB for 6 h caused a substantial inhibition of lysosome acidification that led to the accumulation of non-digestive autophagosomes in macrophages. However, in our previous study, TcdB triggers the formation of acidic autophagic vesicles with an unimpeded autophagic flux at 6 h and induces extensive autophagy-dependent cell death at 24 h in colonic epithelial cells [42]. It is still unclear why different cell types could have different susceptibility to lysosome function exhaustion or response to toxins. In this respect, lysosomes of epithelial cells and macrophages were reported to express different levels of aminopeptidases [43]. The pore-forming toxin listeriolysin O of *Listeria monocytogenes* is also shown to alter the lysosomal integrity in epithelial cells but not in macrophages [44]. It is also notable that, in this study, human monocyte-derived macrophages (THP-1) and murine macrophages (RAW 264.7) reacted similarly to TcdB in terms of SQSTM1/p62 accumulation and cytokine response but exhibited different sensitivities. A recent study also showed that human and murine macrophages showed different sensitivities to lysosomotropic agents [45]. Another important aspect that warrants further investigation is whether TcdB-induced lysosome dysfunction during CDI could instigate other downstream pro-inflammatory pathways, including the AIM2 (absent in melanoma 2)/NLRP3 (NLR family pyrin domain containing 3)-inflammasomes, the CGAS (cyclic GMP-AMP synthase)-STING1 (stimulator of interferon response cGAMP interactor 1) pathway and mitochondrial homeostasis, all of which are important for linking lysosome dysfunction to cytokine
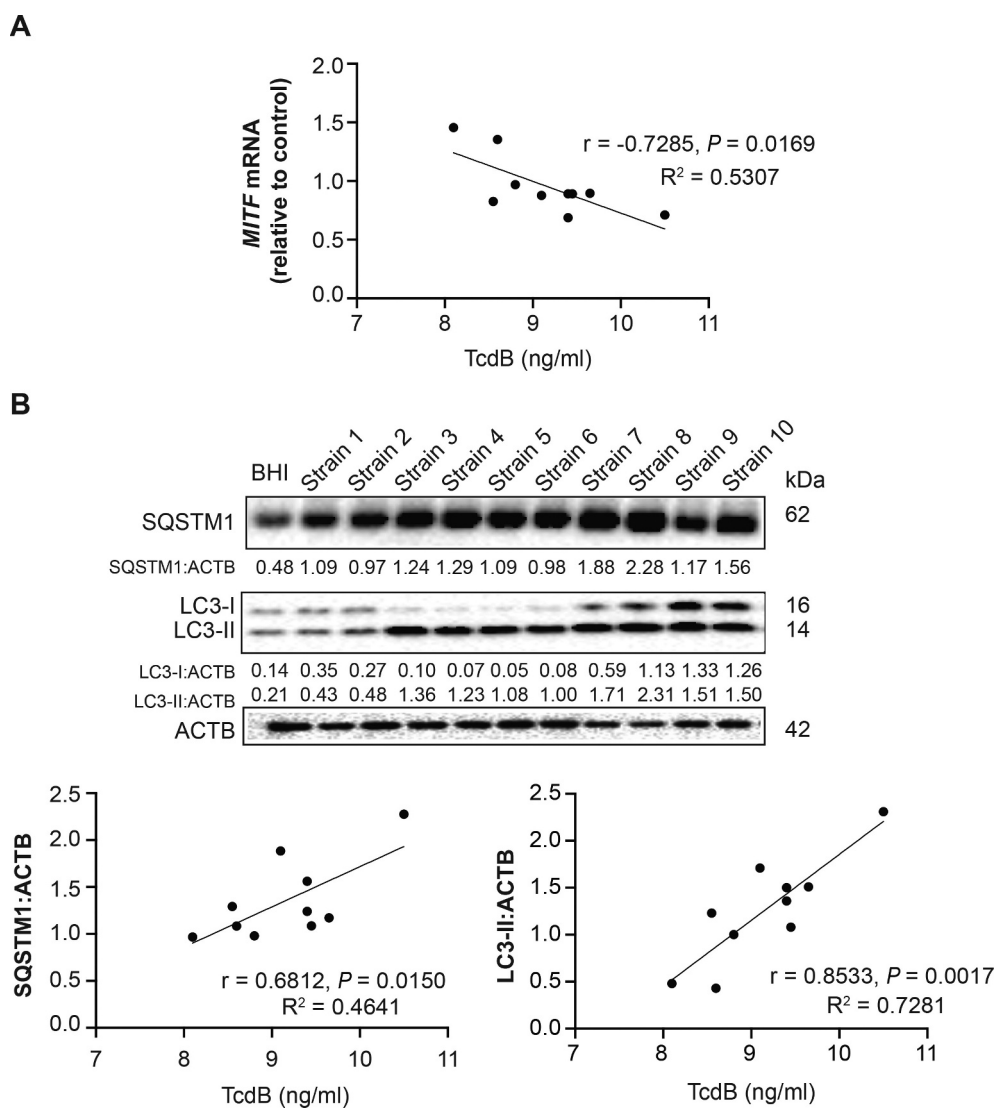
Figure 4. Correlation of *MITF* mRNA expression and autophagic flux impairment with TcdB released from clinical isolates of *C. difficile*. PMA-differentiated THP-1 cells were exposed to the medium of stationary-phase culture of different *C. difficile* clinical isolates (all are ribotype 002) for 6 h. TcdB concentrations were measured by ELISA. (A) Correlation between *MITF* mRNA levels and TcdB concentrations was shown. (B) Correlations between protein levels of autophagic flux markers (LC3-II and SQSTM1/p62; after normalization with ACTB) and TcdB concentrations are shown. Correlation coefficients and *P* values were derived from the Pearson correlation test.

response [23]. In this connection, cytokine response has significant impact on the intestinal epithelial barrier in CDI pathogenesis, in which TcdB-trigged intestinal injury was shown to be attenuated by inhibition of IL1 signaling and genetic ablation of inflammasomes [10].

Concerning the upstream molecular event, it has been demonstrated TcdB could induce colonic epithelial cell death in organoids by inhibiting the WNT signaling [28]. Concordantly, in our study, we showed that TcdB could inhibit the WNT-MITF-lysosome acidification axis in macrophages to mediate the cytokine response. These findings suggest that WNT signaling inhibition by TcdB is of pathological relevance in both colonic epithelial cells and macrophages. Reactivation of the WNT-lysosome pathway would be a potential therapeutic direction in mitigating TcdB-mediated inflammatory response and tissue damage.

Our findings suggest that vitamin D_3 and CBZ restored macrophage lysosome acidification attenuated by TcdB and alleviated the associated symptoms and histological damage in a murine CDI model. In this regard, both agents have been shown to protect against autophagic flux impairment in other pathological conditions. For example, our previous study showed that vitamin D_3, through the PDIA3 (protein disulfide isomerase family A member 3) receptor, could reactivate the autolysosomal degradation function to protect against intracellular *Helicobacter pylori* infection [25]. Other investigators demonstrated that CBZ, an MTOR (mechanistic target of rapamycin kinase)-independent autophagic flux enhancer [30], could prevent the stagnant autophagic flux in the liver of septic mice [46] and alleviate the decreased mitophagic flux caused by defective lysosome acidification in TSC2 (TSC complex subunit 2)-deficient neurons [47]. Although it is thought that the molecular signaling of vitamin D_3 and CBZ
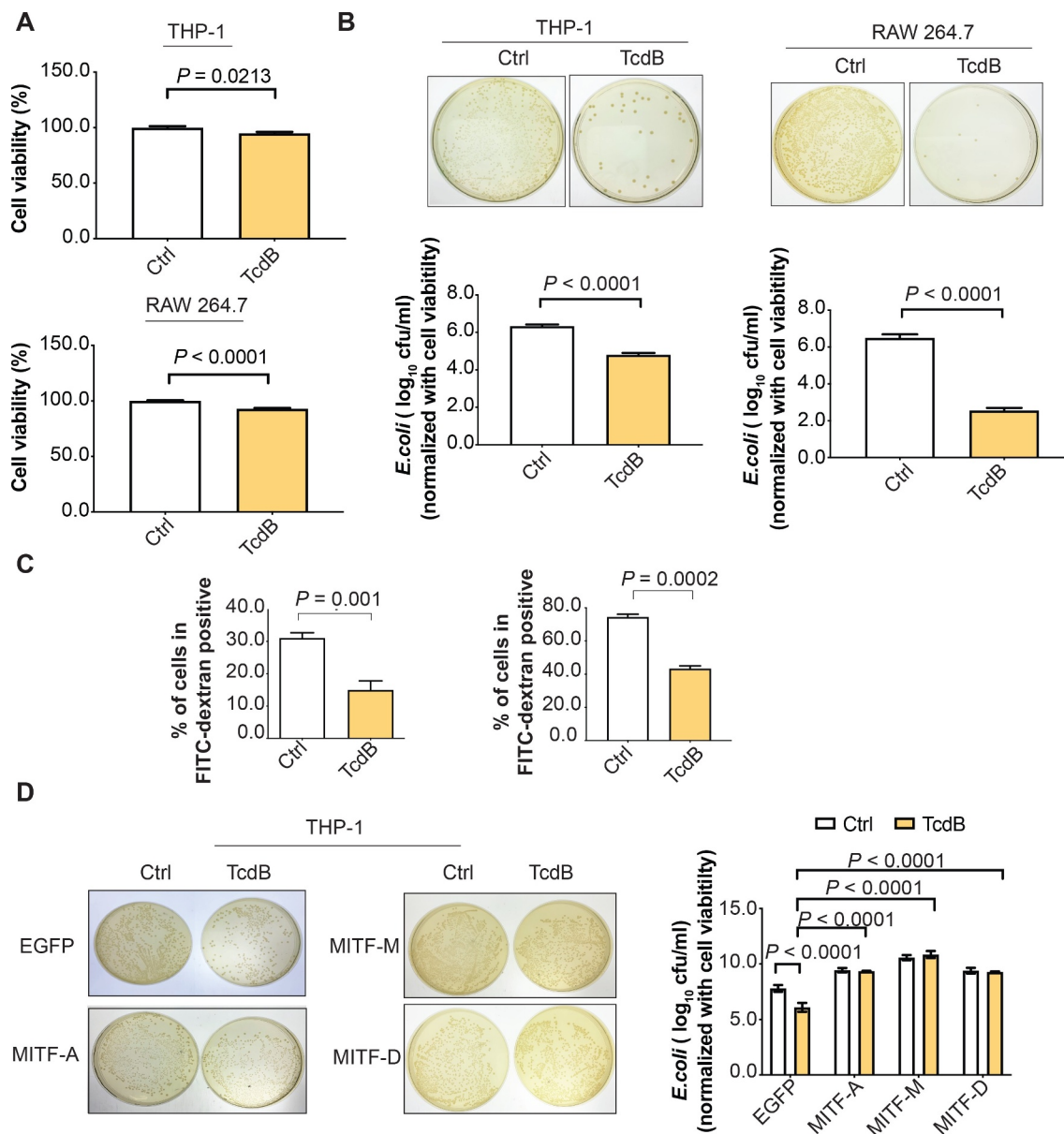
Figure 5. Enforced expression of *MITF* abolished TcdB-impaired phagocytosis. TcdB (10 ng/ml; 6 h) attenuated the (A) cell viability and (B-C) phagocytic activity of THP-1 (PMA-differentiated) and RAW 264.7 macrophages as evidenced by (B) *E. coli* internalization assay and (C) FITC-dextran uptake assay. For the *E. coli* internalization assay, THP-1 and RAW 264.7 were pre-treated with TcdB and then incubated with *E. coli* at 100 MOI for 4 h. Adhered extracellular bacteria were subsequently killed by gentamicin (100 μg/ml). The internalized bacteria were examined by LB agar plating after 24 h. The results of *E. coli* internalization assay were normalized with cell viability. For the FITC-dextran uptake assay, THP-1 and RAW 264.7 macrophages were incubated for 6 h with TcdB and exposed for 1 h to FITC-dextran (250 μg/ml). The fluorescence signals were then analyzed by flow cytometry. (D) THP-1 cells transfected with different isoforms of *MITF* abolished TcdB-mediated inhibition of phagocytosis of *E. coli*. Results are expressed as mean ± S.E.M. from three independent experiments.

are different, our present study indicates that their intracellular signaling could converge on MITF. In this connection, knockdown of *MITF* attenuated the inhibitory effects of 1α,25-dihydroxyvitamin D_3 and CBZ against TcdB-induced expression of *IL1B, IL8* and *CXCL2* in human macrophages (**Fig. S7A-7D**). Whereas the anti-inflammatory effect of vitamin D_3 has been well-established [48], there are only sporadic studies on the anti-inflammatory action of CBZ. To this end, CBZ was reported to reduce the inflammatory exudate in a rat model of inflammatory arthritis [49] and suppress the production of TNF, IL1B, nitric oxide, and prostaglandin E_2 in lipopolysaccharide-stimulated glial cells [50,51]. These findings together with ours support the anti-inflammatory effects

of vitamin D_3 and CBZ in diseases with lysosome dysfunction as a prominent feature. Apart from restoring lysosomal function, we examined the involvement of LC3B-I-to-LC3B-II conversion/autophagosome generation in the anti-inflammatory effects of 1α,25-dihydroxyvitamin D_3 and CBZ. Interestingly, the anti-inflammatory effects of 1α,25-dihydroxyvitamin D_3 and CBZ were abolished after silencing of *BECN1* (beclin 1), *ATG5* (autophagy related 5) and *ATG7* (autophagy related 7) in macrophages (Fig. S7E-7 H). These findings indicated that the protective effects of both agents depend on an unimpeded autophagic flux. In clinical aspects, several studies have investigated the association between the vitamin D serum levels and outcomes of CDI, but the
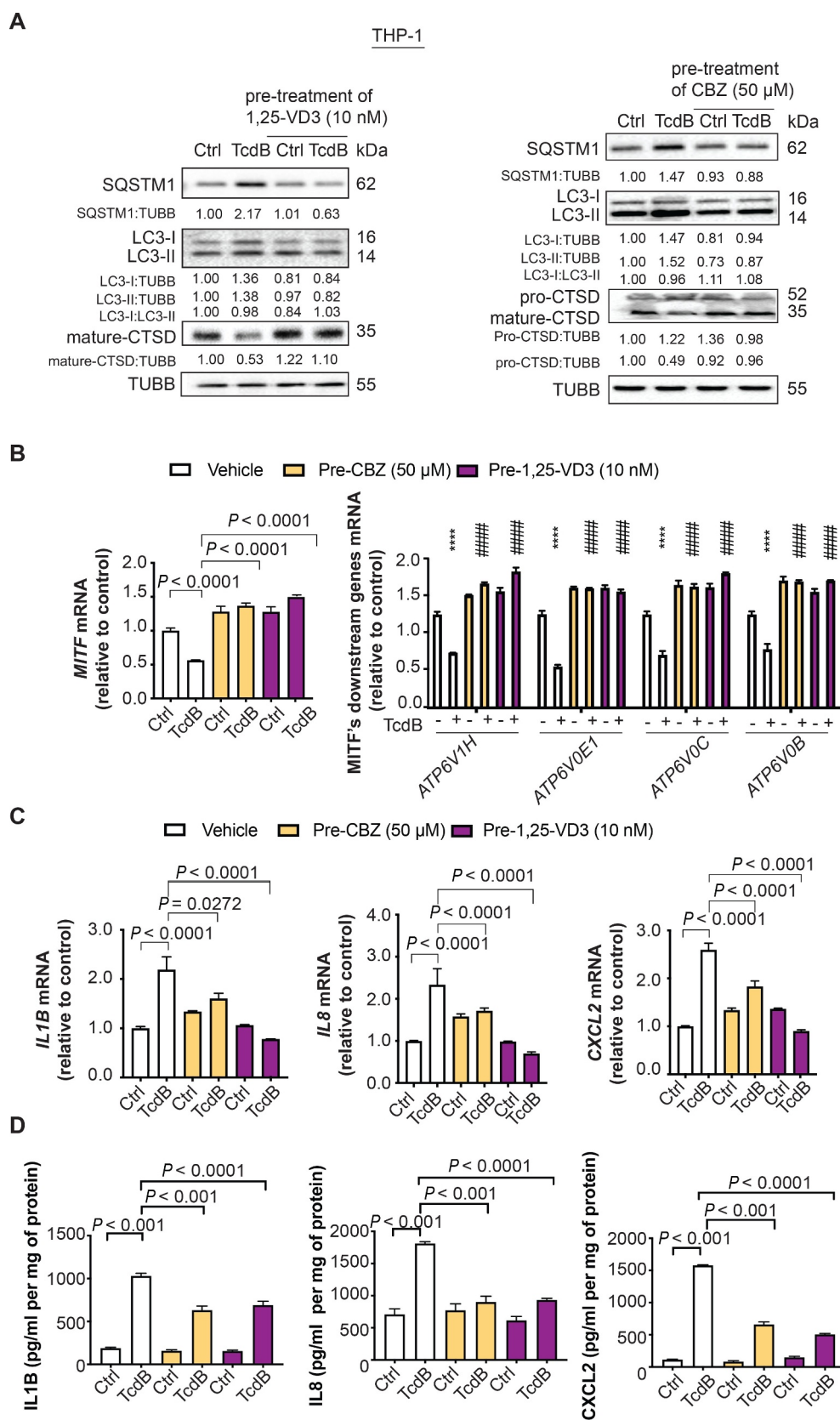
Figure 6. Effects of lysosome activators 1α,25-dihydroxyvitamin D₃ and carbamazepine on TcdB-induced autophagic flux impairment and cytokine response in human PMA-differentiated THP-1 macrophages. Effects of pre-treatment with 1α,25-dihydroxyvitamin D₃ (1,25-VD3) and carbamazepine (CBZ) at the indicated concentrations for 24 h on TcdB (10 ng/ml; 6 h)-induced (A) impairment of autophagic flux and proteolytic cleavage of CTSD; (B) downregulation of mRNA levels of *MITF* and lysosomal proton pump subunits; (C) mRNA expression of pro-inflammatory cytokines in human macrophages are shown. Protein and mRNA levels were quantified by Western blots and RT-qPCR, respectively. (D) Protein levels of pro-inflammatory cytokines in human macrophages were measured by ELISA. Results are expressed as mean ± S.E.M. of 3 independent experiments. ****, $p < 0.0001$ when compared with TcdB-unexposed vehicle control. ####, $p < 0.0001$ when compared with TcdB-exposed vehicle control.
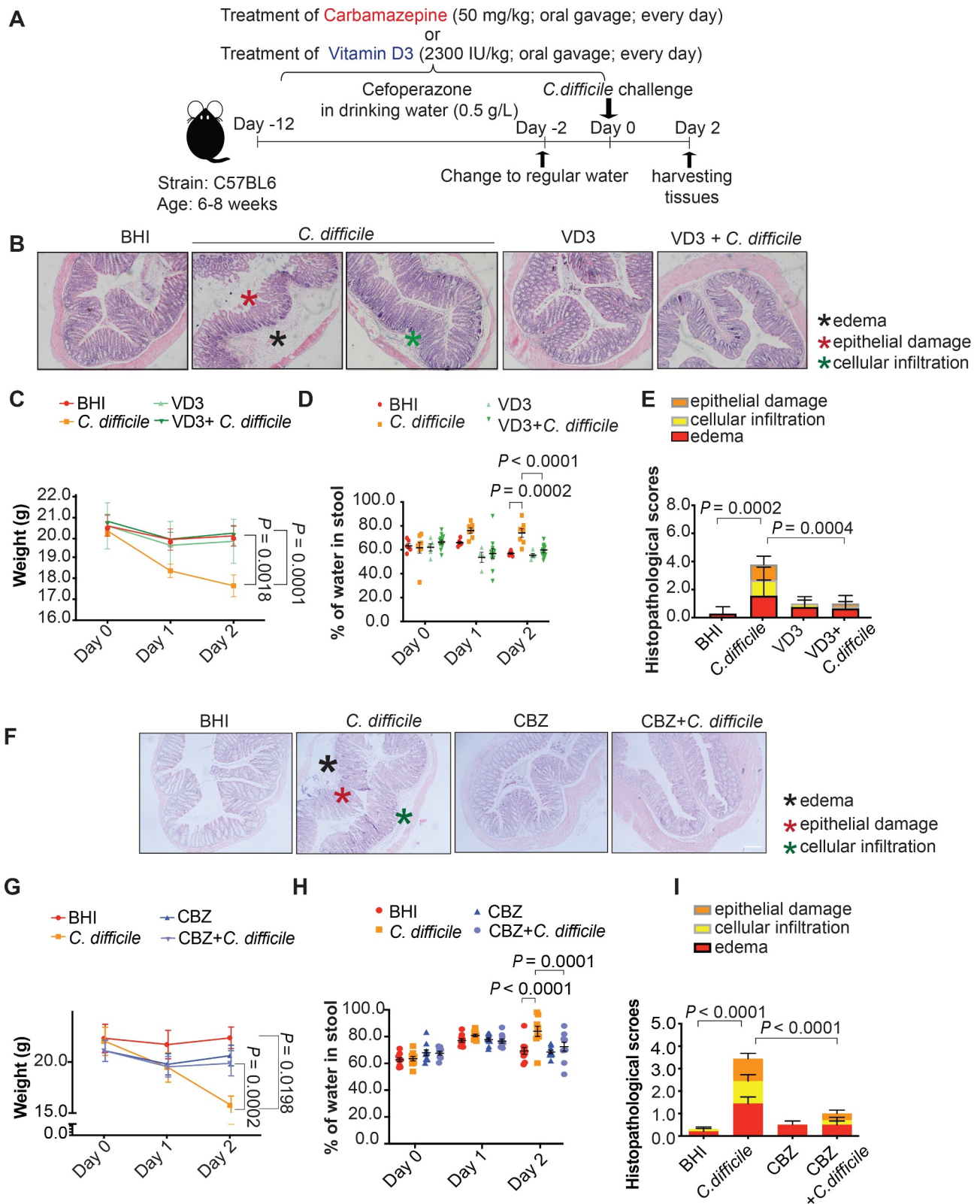
Figure 7. Amelioration of symptoms and histological damage by lysosome activators vitamin D₃ and carbamazepine in a murine CDI model. (A) Mice were given cefoperazone in drinking water (0.5 mg/ml) for 10 days before being challenged with 1×10^8 colony-forming units of a TcdB-hyperproducing *C. difficile* strain (VPI10463) to establish the CDI model. All mice were sacrificed 2 days after CDI. Effects of pre-treatment with (B – E) vitamin D₃ (2300 IU/kg by oral gavage) or (F – I) carbamazepine (CBZ; 50 mg/kg by oral gavage) every other day for 2 weeks before *C. difficile* challenge on (B and F) H&E sections of mice colonic mucosa, (C and G) weight loss, (D and H) severity of diarrhea, and (E and I) histopathological scores of colon tissues 2 days post-infection are shown. Scale bar: 200 μm **, $p < 0.01$; ***, $p < 0.001$; ****, $p < 0.0001$ significantly different between indicated groups (pooled from three batches of experiments; BHI group, n = 10; *C. difficile* group, n = 10; CBZ group, n = 10; *C. difficile* with CBZ group, n = 10; Vitamin D₃ group, n = 5; *C. difficile* with vitamin D₃ group, n = 13).
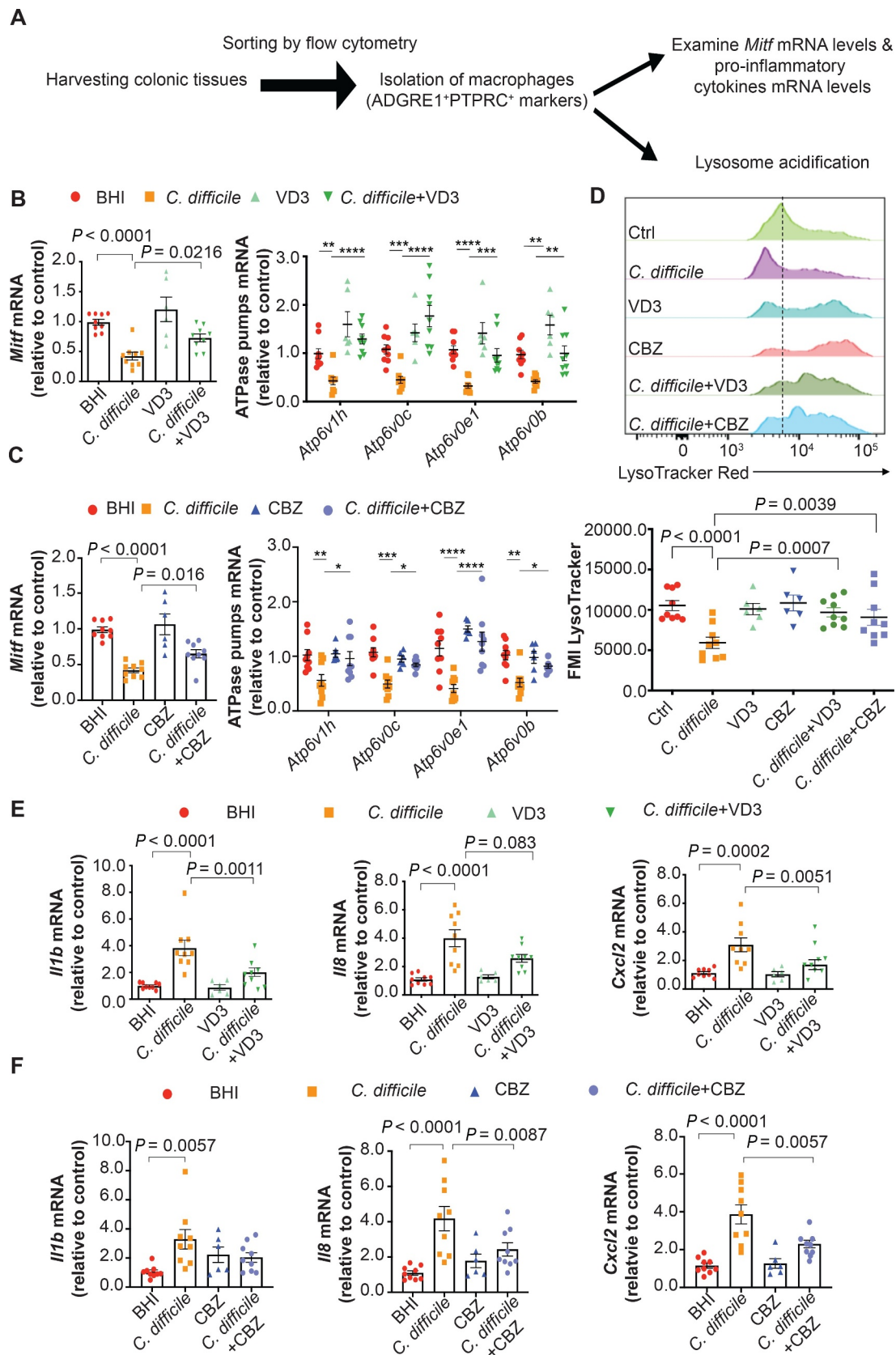
Figure 8. Attenuation of *Mitf* downregulation, lysosome dysfunction, and pro-inflammatory cytokine expression in colonic macrophages by vitamin D_3 and carbamazepine in the murine CDI model. (A) Workflow of isolation of colonic macrophages is shown. (B-C) Effects of CDI without or with pre-treatment of (B) vitamin D_3 (VD3; 2300 IU/kg by oral gavage) and (C) carbamazepine (CBZ; 50 mg/kg by oral gavage) every other day for 2 weeks on mRNA expression of *MITF* and the four lysosomal proton pump subunits in isolated colonic macrophages are shown (pooled from three batches of experiments; BHI group, n = 9; *C. difficile* group, n = 9; CBZ or VD3 group, n = 6 each; *C. difficile* with CBZ or VD3 group, n = 9 each). (D) Effects of CDI without or with pre-treatment of vitamin D_3 or carbamazepine on mean fluorescence intensity (MFI) of LysoTracker Red staining in isolated colonic macrophages are shown. (E-F) Effects of CDI without or with pre-treatment of (E) vitamin D_3 and (F) carbamazepine on mRNA expression of *Il1b*, *Il8* and *Cxcl2* in isolated colonic macrophages are shown.
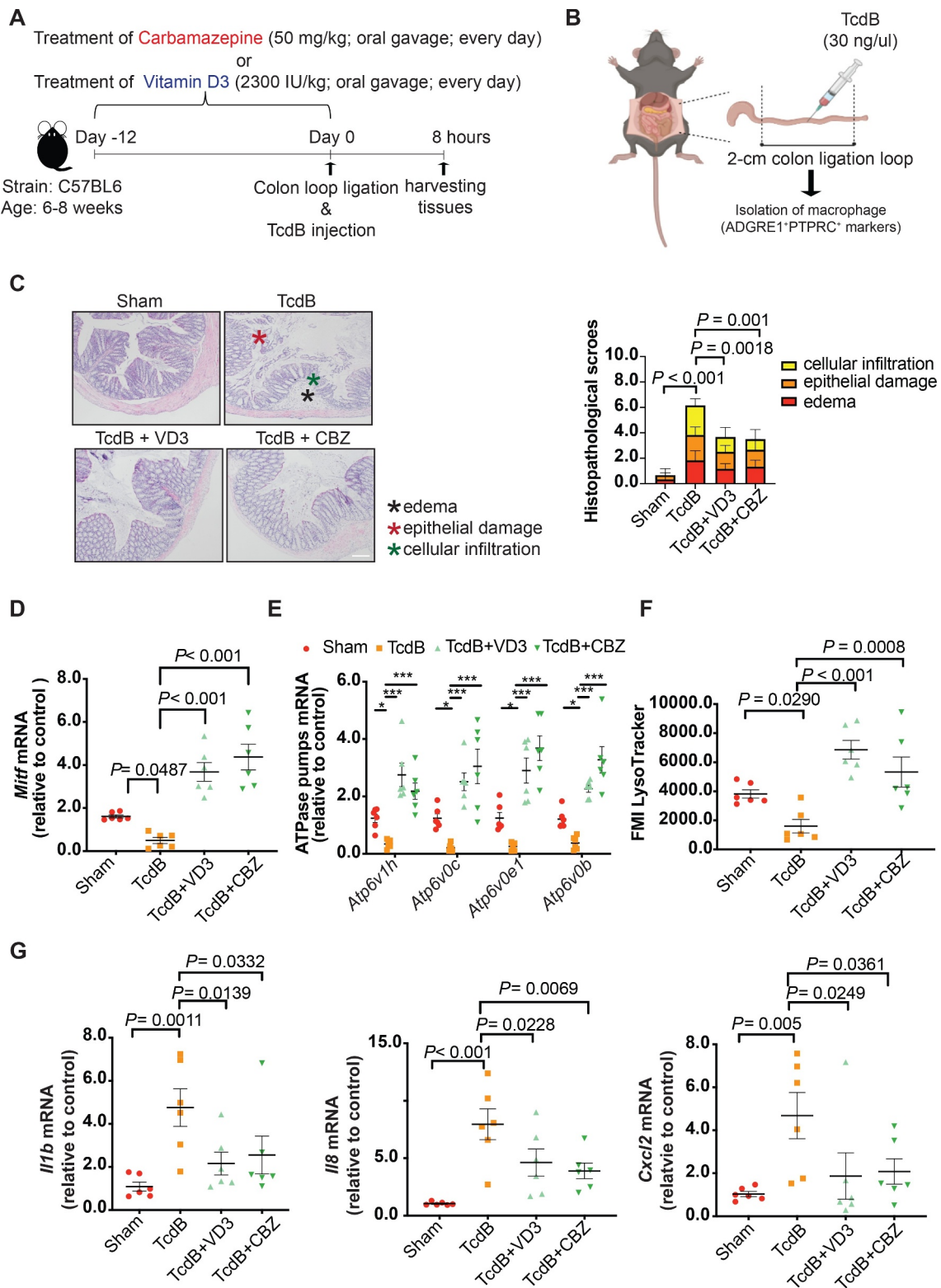
Figure 9. Attenuation of *Mitf* downregulation, lysosome dysfunction, and pro-inflammatory cytokine expression in colonic macrophages by vitamin D_3 and carbamazepine in the murine colon loop ligation model. (A) Workflow of pre-treatment with lysosome activators in the colon loop ligation model is shown. (B) A schematic illustration of the colon loop ligation model. (C) Histopathological scores of sealed colon segment tissues. Scale bar: 200 μm (D-E) mRNA expression of *Mitf* and the four lysosomal proton pump subunits in isolated colonic macrophages are shown. (F) Effects of TcdB without or with pre-treatment of vitamin D_3 (VD3) or carbamazepine (CBZ) on mean fluorescence intensity (MFI) of LysoTracker Red staining in isolated colonic macrophages are shown. (G) Effects of TcdB without or with pre-treatment with vitamin D_3 or carbamazepine on mRNA expression of *Il1b, Il8* and *Cxcl2* in isolated colonic macrophages are shown. **, $p < 0.01$; ***, $p < 0.001$ significantly different between indicated groups (pooled from three batches of experiments; Sham group, n = 6; TcdB group, n = 6; TcdB with CBZ or VD3 group, n = 6 each).

conclusion is still controversial. Some reported that higher serum level of 25-hydroxyvitamin D_3 was associated with a shorter duration of diarrhea in CDI patients [52]. Similarly, higher plasma level of 25-hydroxyvitamin D_3 was linked to reduced CDI mortality among patients with inflammatory bowel disease [53]. However, another study demonstrated that low serum 25-hydroxyvitamin D_3 level is not associated with adverse CDI outcomes [54]. The inconsistency may be attributed to the difference in co-morbidities in the studied cohorts. Further investigation is required.

Currently, patients with CDI are treated with vancomycin or metronidazole. However, the emergence of multi-drug resistant *C. difficile* has posed a rising concern [55,56]. Therefore, development of non-antibiotic approaches to treat CDI is an area of active investigation. In this study, our data provide the first evidence that TcdB produced by *C. difficile* could downregulate *MITF* to cause macrophage lysosome dysfunction, which triggered a heightened inflammatory response in CDI. Therapeutically, restoration of lysosomal function by lysosome activators could serve as a potential strategy for managing CDI patients. In this regard, both vitamin D_3 and carbamazepine have been widely used to treat other diseases. Their potential therapeutic effects in CDI should be further assessed with clinical trials to determine if these agents could act synergistically with existing treatments to improve the clinical outcomes of CDI patients.

Materials and methods

Reagents and antibodies

Primary antibodies we used were anti-LC3B (Novus Biologicals, NB100-2220), anti-LC3B (Cell Signaling Technology, 3868S), anti-SQSTM1 (BD Biosciences, 610,832), anti-CTSD (Santa Cruz Biotechnology, SC-6487), anti-ACTB (Cell Signaling Technology, 4967S), anti-LAMP1 (Cell Signaling Technology, 9091S), anti-phospho-NFKB RELA/p65 (Ser536; Cell Signaling Technology, 3033), anti-NFKB RELA/p65 (Cell Signaling Technology, 8242), anti-NFKBIA/IKBα (Cell Signaling Technology, 4814), anti-MITF (Cell Signaling Technology, 12,590), anti-TUBB/β-Tubulin (Cell Signaling Technology, 2146), anti-non-phospho (active)-CTNNB1/β-Catenin (Ser45; Cell Signaling Technology, 19,807), anti-LEF1 (Cell Signaling Technology, 2230), anti-TCF7L2 (ABclonal, A19548), and anti-CTNNB1/β-catenin (Cell Signaling Technology, 8480). Secondary antibodies used included anti-mouse conjugated to horseradish peroxidase (Sigma-Aldrich, A2304) and anti-rabbit conjugated to horseradish peroxidase (GE Healthcare, NA9340) for Western blots; anti-rabbit conjugated to Alexa Fluor 568 (A11011), anti-mouse conjugated to Alexa Fluor 568 (A11031), and anti-mouse conjugated to Alexa Fluor 488 (A21202) for confocal microscopy were from Life Technology.

Pharmacological agents: 1α,25-dihydroxyvitamin D_3 (D1530), vitamin D_3 (C9756), bafilomycin A_1 (B1793), rapamycin (37,094), carbamazepine (C4024) and cefoperazone sodium salt (C4292) were purchased from Sigma-Aldrich.

Bacterial Toxins: TcdA was purchased from Native Antigen (CDA-TNL). TcdB was purchased from Cayman

Chemical (19,665). Lipopolysaccharide (LPS) was purchased from Sigma-Aldrich (L2018).

ELISA kits: TcdB (Mlbio, CDT-B), human IL1B (Wuhan Fine Biotech Co., EH0185), human IL8 (Cloud-clone corp, SEQ080Hu), human CXCL2 (C-X-C motif chemokine ligand 2; Cloud-clone corp, SEB603 Hu), mouse IL1B (Thermo Fisher Scientific, BMS6002), mouse IL8 (Wuhan Fine Biotech Co., EM1592), and mouse CXCL2 (Cloud-clone corp, SEB603Mu).

Human macrophage culture

The human monocytic cell line THP-1 and murine macrophage cell line RAW 264.7 were obtained from the American Type Culture Collection (ATCC, TIB-202 for THP-1; TIB-71 for RAW 264.7). THP-1 and RAW 264.7 cells were cultured in RPMI-1640 (Gibco™, Thermo Fisher Scientific, 21,875,034), and Dulbecco's Modified Eagle's Medium (DMEM; Thermo Fisher Scientific, 11,965,092), respectively, supplemented with 10% fetal bovine serum (FBS; Gibco™, Thermo Fisher, 26,140,079) and 1% penicillin-streptomycin (Gibco™, Thermo Fisher, 15,070,063) at 37°C in 5% CO_2. For inducing macrophage differentiation, THP-1 cells were stimulated with 100 nM phorbol 12-myristate 13-acetate (PMA; Sigma-Aldrich,P8319) for 24 h. Afterward, differentiated THP-1 were cultured in fresh RPMI-1640 for the experiments.

Western blots

Cells or tissues were harvested and washed with ice-cold phosphate-buffered saline (PBS; 137 mM NaCl, 2.7 mM KCl, 10 mM Na_2HPO_4, 1.8 mM KH_2PO_4, pH 7.6), and lysed in immunoprecipitation assay buffer. Cellular debris was pelleted by centrifugation at $13,000 \times g$ for 30 min at 4°C. The protein concentrations of the total lysate were measured using a standard Bradford assay (Bio-Rad, 5,000,122,). For Western blots, 10 µg of protein from the total cell lysate was electrophoresed by SDS–PAGE. The proteins were then transferred to nitrocellulose membrane (Bio-Rad, 1,620,177) and probed with primary antibodies followed by horseradish peroxidase-labeled secondary antibodies. Proteins were visualized using enhanced chemiluminescence (Cell Signaling Technology, 7003S) and imaged by the digital a Western blot imaging system (Bio-Rad, CUHK instruments). Band intensity was quantified by the ImageJ software. Western blots from independent batches of experiments and their quantitative analysis by densitometry were shown in (Data S1 to Data S4).

Reverse transcription-quantitative PCR

Total RNA was extracted by TRIzol and then reverse-transcribed into complementary DNA by a PrimeScript™ RT reagent Kit (TakaRa, RR037B). mRNA expression of pro-inflammatory cytokines, chemokines as well as MITF/TFEB family and downstream genes of MITF was measured by quantitative PCR with SYBR Pre-mix Ex Taq kit (TakaRa, RR820B) using the primers shown in Table S1. 28S rRNA was used as internal control. The relative mRNA expression levels were calculated by the delta-delta C_T method.

Confocal laser scanning microscopy

Cells were seeded on coverslips until 70% confluence. Treated cells were then fixed with 4% formaldehyde solution for 30 min at room temperature. After fixation, cells were washed twice with PBS and incubated with the blocking buffer (5% FBS in PBS with 0.25% Triton X-100 [Sigma-Aldrich, T8787]) for 60 min and subsequently incubated with primary antibody overnight. Afterward, slips were incubated with secondary antibody for 60 min at room temperature. Images were captured by a confocal microscope (Leica) and analyzed using the ImageJ software.

Transmission election microscopy

Cells were fixed for 1 h at 4°C in 1.6% glutaraldehyde in 0.1 mol/L phosphate buffer, pH 7.2, then washed and fixed again in aqueous 2% osmium tetroxide, dehydrated in ethanol, embedded in Epon (Serva, 21,045.02), and processed for electron microscopy with a Zeiss EM 902 transmission electron microscope at 80 kV. Ultra-thin sections were cut and stained with uranyl acetate and lead citrate.

RNA interference

Cells were seeded at 1×10^5 cells per well in 6-well plates prior to the transfection. During the transfection, the cells were transfected with small interfering RNA (Thermo Fisher) specific for *SQSTM1* (127,334), *ATG5* (18,160), *ATG7* (135,754), *BECN1* (137,199) and *MITF* (110,566) using the jetPRIME transfection reagent (Polyplus, 114–15) according to the manufacturer's protocol.

Assay for LC3⁺ autophagic vacuoles by mCherry-GFP-LC3 plasmid

Cells were grown on glass chamber slides overnight and then transfected with a plasmid encoding mCherry-GFP-LC3 for 24 h. After transfection, cells were exposed to TcdB (10 ng/mL) for 6 h. Cells were then rinsed twice with 1× PBS and fixed in 4% paraformaldehyde for 15 min at room temperature. After rinsing twice with 1× PBS, the slides were mounted in prolong gold anti-fade reagent (Invitrogen, P36930) and then analyzed under a confocal microscope (Leica).

Assays for lysosome enzyme activities

Cells (1×10^5) were seeded in 60-mm plates and were pre-treated with 1α,25-dihydroxyvitamin D_3 or carbamazepine at the indicated concentrations for 24 h before the exposure to TcdB (10 nM). Cellular debris was pelleted by centrifugation at $13,000 \times g$ for 30 min at 4°C. The total lysate protein were used to detect lysosomal enzyme activities using the Acid Phosphatase Assay Kit (Sigma-Aldrich, CS0740) and the β-N-Acetylglucosaminidase Assay Kit (Sigma-Aldrich, CS0780).

Overexpression of MITF

Cells were grown on glass chamber slides (Thermo Fisher Scientific, 171,080) overnight and then transfected with pEGFP-N1 (Addgene, 6085–1), pEGFP-N1-MITF-M (Addgene, 38,131; deposited by Shawn Ferguson), pEGFP-N1-MITF-A (Addgene, 38,132; deposited by Shawn Ferguson) or pEGFP N1-MITF-D (Addgene, 38,133; deposited by Shawn Ferguson) for 24 h. After transfection, cells were exposed to TcdB (10 ng/mL) for 6 h.

Luciferase transcriptional activation assay

Cells were grown on glass chamber slides overnight and then transfected with pGL3-MITF plasmid (Hitrobio Biotechnology; customized plasmid construction) for 24 h. After transfection, cells were exposed to TcdB (10 ng/mL) for 6 h and the cells were lysed. The luciferase activity was determined in accordance with the instructions (Dual-luciferase Reporter Assay System; Promega, E1980).

Chromatin immunoprecipitation coupled with next-generation sequencing

ChIP was performed using Magna ChIP A/G kit (Millipore, 17–10,085/86) following the manufacturer's instructions. In general, formaldehyde-fixed control and TcdB-exposed THP-1 macrophages were lysed and subject to sonication to obtain DNA fragments ranging from 300–600 bp. Sheared and cleared chromatin were incubated overnight with 5 µg of MITF (D5G7V) antibody (Cell Signaling Technology, 12,590) or anti-IgG antibody (Santa Cruz Biotechnology, sc-2027). Antibody-protein complexes were immunoprecipitated with Magna ChIP A/G beads, washed, eluted and reverse-crosslinked and treated with proteinase K (Thermo Fisher Scientific, 25,530,049). Library construction was performed using an NEB kit (New England Biolabs, E7645) and sequenced on the Illumina HiSeq X Ten. All sequence reads were mapped using Bowtie 2 onto the hg38 USCS reference human genome. MACS2 was used to call peaks with the sonicated input as a control and an initial threshold q-value of 0.01 as the cutoff. Visualization of read count data was performed by converting raw bam files to bigwig files using IGV tools. ChIP seeker was used to analyze binding data.

Animals and housing

C57BL/6 mice were maintained at the Laboratory Animal Services Center of the Prince of Wales Hospital and housed under 12-hour light/dark cycles in a pathogen-free room with clean bedding and free access to food and water. Cage and bedding changes were performed each week. Throughout the experiment, the mice were assessed daily with moribund animals humanely euthanized by CO_2 asphyxiation followed by cervical dislocation. All animal studies were performed in accordance with a protocol (20–085-NSF and 20–084-MIS) approved by the Animal Experimentation Ethics Committee of the Chinese University of Hong Kong.

Isolation of colonic macrophages

Macrophages were isolated from colonic tissues according to a published protocol [57]. Briefly, the colon tissues were minced into a 1.5-cm pieces and washed with warm Ca^{2+} and Mg^{2+}-free PBS. Afterward, the samples were treated with pre-warmed 2 mM EDTA in Ca^{2+} and Mg^{2+}-free HBSS (Thermo Fisher Scientific, 88,284) with 2% FBS for 20 min at 37°C to remove the epithelial layer. For digestion of intestinal tissue, the samples were digested in pre-warm collagenase VIII (Sigma-Aldrich, C2139), DNAse I (Sigma-Aldrich, 4,536,282,001) solution for 20 min at 37°C and then centrifuged at $250 \times g$ for 5 min. For antibody staining, cell pellets were incubated in the flow cytometry staining buffer and incubated with 2.5 ug purified anti-mouse F4/80 antibody (Biolegend, 157,310) and anti-mouse PTPRC/CD45 (Biolegend, 103,155) for 30 min on ice. For storing, 3×10^5 cells were isolated and washed once with PBS and then sorted by a BD FACSAria Fusion Flow cytometer. All data and figures were analyzed and created using the FlowJo Software.

Murine CDI model and histological assessment

A previously published CDI model was employed [58]. Briefly, male mice of 6- to 8-weeks old were given cefoperazone in drinking water at a concentration of 0.5 mg/ml for 10 days (from day −12 to day −2). Afterward, the drinking water was switched to regular sterilized water for the remainder of the experiment. On day 0, mice were challenged with 1×10^8 colony-forming units of vegetative *C. difficile* (strain VPI10463, Genotype: TcdA+, TcdB++, Ribotype 087, ATCC 43255) by oral gavage. For the lysosome activator (vitamin D_3 and carbamazepine) prophylaxis groups, mice were pre-treated with vitamin D_3 (2300 IU/kg by oral gavage) or carbamazepine (CBZ; 50 mg/kg by oral gavage) every other day for 2 weeks before *C. difficile* challenge. The doses of vitamin D_3 (high dose relative to human level) and CBZ used in the present study were referred to previous studies [51,59,60]. Animals infected with *C. difficile* were monitored daily for signs and symptoms of diarrhea, wet tails, hunched posture, and weight loss. All animals were sacrificed 2 days post-infection. Fecal samples were collected on day 0, 1 and 2 to evaluate the stool water content as an indicator of diarrhea as previously reported [61]. Besides, fecal samples on day 2 were collected for enumeration of total *C. difficile* colony-forming units (CFU) on the chromID *C. difficile* agar (Biomerieux, 43,871). Colonic tissues were fixed for histological examination. Histological sections were stained with hematoxylin and eosin (H&E) and scored according to criteria previously described, namely edema, cellular infiltration and epithelial damage, to examine the influence of CDI on colonic tissues [62]. The scores were rated by two researchers.

Colon loop ligation assay

Male mice of 6- to 8-weeks old were used in the experiments. Mice were anaesthetized following overnight fasting. The ascending colon was located and sealed with a 2 cm loop with silk ligatures. Forty microliter of TcdB in normal saline (30 ng/μl) or the same volume of normal saline were injected through a LV catheter into the sealed colon segment and then the wounds were closed with stitches. Mice were allowed to recover for 8 h before harvesting the ligated colon segments. The colon segments were fixed for H&E staining and histological score analysis as well as subject to macrophage isolation. For the lysosome activator (vitamin D_3 and carbamazepine) prophylaxis groups, mice were pre-treated with vitamin D_3 or carbamazepine as described above every other day for 2 weeks before the colon loop ligation assay.

Statistical analysis

Statistical analyses were performed using Prism 8 software. For datasets with normal distribution, multiple comparisons were performed using one-way ANOVA with Tukey's post hoc analysis. The parametric Student t-test was used to compare two groups of data with normal distribution. Data are presented as the mean values ± standard error mean (S.E.M.) unless stated otherwise. Statistical significance was defined as a *p*-value < 0.05, in which * represents a significant difference, at least *p* < 0.05.

Disclosure statement

No potential conflict of interest was reported by the author(s).

ORCID

Margaret Ip http://orcid.org/0000-0003-1291-6537
Sunny Hei Wong http://orcid.org/0000-0002-3354-9310

References

[1] Marra AR, Perencevich EN, Nelson RE, et al. Incidence and outcomes associated with clostridium difficile infections. JAMA Network Open. 2020;3:e1917597.

[2] Wiegand PN, Nathwani D, Wilcox MH, et al. Clinical and economic burden of Clostridium difficile infection in Europe: a systematic review of healthcare-facility-acquired infection. J Hosp Infect. 2012;81:1–14.

[3] Ho J, Dai RZ, Kwong TN, et al. Disease Burden of Clostridium difficile infections in Adults, Hong Kong, China, 2006-2014. Emerg Infect Dis. 2017;23:1671–1679.

[4] McKee HK, Kajiwara C, Yamaguchi T, et al. Clostridioides difficile toxins enhanced the in vitro production of CXC chemokine ligand 2 and tumor necrosis factor-alpha via Toll-like receptors in macrophages. J Med Microbiol. 2021;70. DOI:10.1099/jmm.0.001342.

[5] Goy SD, Olling A, Neumann D, et al. Human neutrophils are activated by a peptide fragment of Clostridium difficile toxin B presumably via formyl peptide receptor. Cell Microbiol. 2015;17:893–909.

[6] Markham NO, Bloch SC, Shupe JA, et al. Murine intrarectal instillation of purified recombinant clostridioides difficile toxins enables mechanistic studies of pathogenesis. Infect Immun. 2021;89. DOI:10.1128/IAI.00543-20.

[7] Abt MC, McKenney PT, Pamer EG. Clostridium difficile colitis: pathogenesis and host defence. Nat Rev Microbiol. 2016;14:609–620.

[8] Souza MH, Melo-filho AA, Rocha MFG, et al. The involvement of macrophage-derived tumour necrosis factor and lipoxygenase products on the neutrophil recruitment induced by Clostridium difficile toxin B. Immunology. 1997;91:281–288.

[9] Rocha MF, Maia ME, Bezerra LR, et al. Clostridium difficile toxin A induces the release of neutrophil chemotactic factors from rat peritoneal macrophages: role of interleukin-1beta, tumor necrosis factor alpha, and leukotrienes. Infect Immun. 1997;65(7):2740–2746.

[10] Ng J, Hirota SA, Gross O, et al. Clostridium difficile toxin-induced inflammation and intestinal injury are mediated by the inflammasome. Gastroenterology. 2010;139:542–552, 552 e541-543.

[11] Xu H, Yang J, Gao W, et al. Innate immune sensing of bacterial modifications of Rho GTPases by the Pyrin inflammasome. Nature. 2014;513:237–241.

[12] Jefferson KK, Smith MF Jr., Bobak DA. Roles of intracellular calcium and NF-kappa B in the Clostridium difficile toxin A-induced up-regulation and secretion of IL-8 from human monocytes. J Immunol. 1999;163:5183–5191.

[13] Chen P, Tao L, Liu Z, et al. Structural insight into Wnt signaling inhibition by Clostridium difficile toxin B. FEBS J. 2019;286:874–881.

[14] El Feghaly RE, Stauber JL, Deych E, et al. Markers of intestinal inflammation, not bacterial burden, correlate with clinical outcomes in Clostridium difficile infection. Clin Infect Dis. 2013;56:1713–1721.

[15] Solomon K, Martin AJ, O'Donoghue C, et al. Mortality in patients with Clostridium difficile infection correlates with host pro-inflammatory and humoral immune responses. J Med Microbiol. 2013;62:1453–1460.

[16] Wang H, Wang N, Xu D, et al. Oxidation of multiple MiT/TFE transcription factors links oxidative stress to transcriptional control of autophagy and lysosome biogenesis. Autophagy. 2020;16:1683–1696.

[17] Zhang T, Zhou Q, Ogmundsdottir MH, et al. Mitf is a master regulator of the v-ATPase, forming a control module for cellular homeostasis with v-ATPase and TORC1. J Cell Sci. 2015;128:2938–2950.

[18] Leclerc J, Garandeau D, Pandiani C, et al. Lysosomal acid ceramidase ASAH1 controls the transition between invasive and proliferative phenotype in melanoma cells. Oncogene. 2019;38:1282–1295.

[19] Vohra P, Poxton IR. Induction of cytokines in a macrophage cell line by proteins of Clostridium difficile. FEMS Immunol Med Microbiol. 2012;65:96–104.

[20] Castagliuolo I, Keates AC, Wang CC, et al. Clostridium difficile toxin A stimulates macrophage-inflammatory protein-2 production in rat intestinal epithelial cells. J Immunol. 1998;160:6039–6045.

[21] Dorrington MG, Fraser IDC. NF-kappaB signaling in macrophages: dynamics, crosstalk, and signal integration. Front Immunol. 2019;10:705.

[22] Duran A, Linares JF, Galvez AS, et al. The signaling adaptor p62 is an important NF-kappaB mediator in tumorigenesis. Cancer Cell. 2008;13:343–354.

[23] Wu WKK, Yue J. Autophagy in host-microbe interactions. Semin Cell Dev Biol. 2020;101:1–2.

[24] Klionsky DJ, et al. Guidelines for the use and interpretation of assays for monitoring autophagy. 4th. Autophagy2021 1–382 . DOI: 10.1080/15548627.2020.1797280.

[25] Hu W, Zhang L, Li MX, et al. Vitamin D3 activates the auto-lysosomal degradation function against Helicobacter pylori through the PDIA3 receptor in gastric epithelial cells. Autophagy. 2019;15:707–725.

[26] Mandic LM, Acimovic JM, Jovanovic VB. The possibility of determining N-acetyl-beta-D-glucosaminidase isoenzymes under alkaline conditions. Clin Biochem. 2005;38:384–389.

[27] Sun P, Sleat DE, Lecocq M, et al. Acid phosphatase 5 is responsible for removing the mannose 6-phosphate recognition marker from lysosomal proteins. Proc Natl Acad Sci U S A. 2008;105:16590–16595.

[28] Tao L, Zhang J, Meraner P, et al. Frizzled proteins are colonic epithelial receptors for C. difficile toxin B. Nature. 2016;538:350–355.

[29] Wong CO, Gregory S, Hu H, et al. Lysosomal degradation is required for sustained phagocytosis of bacteria by macrophages. Cell Host Microbe. 2017;21:719–730 e716.

[30] Sarkar S, Ravikumar B, Floto RA, et al. Rapamycin and mTOR-independent autophagy inducers ameliorate toxicity of polyglutamine-expanded huntingtin and related proteinopathies. Cell Death Differ. 2009;16:46–56.

[31] Hutton ML, Mackin KE, Chakravorty A, et al. Small animal models for the study of Clostridium difficile disease pathogenesis. FEMS Microbiol Lett. 2014;352:140–149.

[32] Gao W, Yang J, Liu W, et al. Site-specific phosphorylation and microtubule dynamics control Pyrin inflammasome activation. Proc Natl Acad Sci U S A. 2016;113:E4857–4866.

[33] Orrell KE, Melnyk RA. Large clostridial toxins: mechanisms and roles in disease. Microbiol Mol Biol Rev. 2021;85:e0006421.

[34] Orr ME, Oddo S. Autophagic/lysosomal dysfunction in Alzheimer's disease. Alzheimers Res Ther. 2013;5:53.

[35] Senkevich K, Gan-Or Z. Autophagy lysosomal pathway dysfunction in Parkinson's disease; evidence from human genetics. Parkinsonism Relat Disord. 2020;73:60–71.

[36] Wang X, Zhang X, Chu ESH, et al. Defective lysosomal clearance of autophagosomes and its clinical implications in nonalcoholic steatohepatitis. FASEB J. 2018;32:37–51.

[37] Hu W, Chan H, Lu L, et al. Autophagy in intracellular bacterial infection. Semin Cell Dev Biol. 2020;101:41–50.

[38] Zhang L, Hu W, Cho CH, et al. Reduced lysosomal clearance of autophagosomes promotes survival and colonization of Helicobacter pylori. J Pathol. 2018;244:432–444.

[39] Ho J, Yu J, Wong SH, et al. Autophagy in sepsis: degradation into exhaustion? Autophagy. 2016;12:1073–1082.

[40] Riesenberg S, Groetchen A, Siddaway R, et al. MITF and c-Jun antagonism interconnects melanoma dedifferentiation with pro-inflammatory cytokine responsiveness and myeloid cell recruitment. Nat Commun. 2015;6:8755.

[41] Qian L, Pan S, Shi L, et al. Downregulation of microRNA-218 is cardioprotective against cardiac fibrosis and cardiac function impairment in myocardial infarction by binding to MITF. Aging (Albany NY). 2019;11:5368–5388.

[42] Chan H, Zhao S, Zhang L, et al. Clostridium difficile toxin B induces autophagic cell death in colonocytes. J Cell Mol Med. 2018;22:2469–2477.

[43] Yayoi Y, Ohsawa Y, Koike M, et al. Specific localization of lysosomal aminopeptidases in type II alveolar epithelial cells of the rat lung. Arch Histol Cytol. 2001;64:89–97.

[44] Malet JK, Cossart P, Ribet D. Alteration of epithelial cell lysosomal integrity induced by bacterial cholesterol-dependent cytolysins. Cell Microbiol. 2017;19:e12682.

[45] Ohlinger K, Absenger-Novak M, Meindl C, et al. Different sensitivity of macrophages to phospholipidosis induction by amphiphilic cationic drugs. Int J Mol Sci. 2020;21:8391.

[46] Lin CW, Lo S, Perng D-S, et al. Complete activation of autophagic process attenuates liver injury and improves survival in septic mice. Shock. 2014;41:241–249.

[47] Ebrahimi-Fakhari D, Saffari A, Wahlster L, et al. Impaired mitochondrial dynamics and mitophagy in neuronal models of tuberous sclerosis complex. Cell Rep. 2016;17:1053–1070.

[48] Yin K, Agrawal DK. Vitamin D and inflammatory diseases. J Inflamm Res. 2014;7:69–87.

[49] Bianchi M, Rossoni G, Sacerdote P, et al. Carbamazepine exerts anti-inflammatory effects in the rat. Eur J Pharmacol. 1995;294:71–74.

[50] Matoth I, Pinto F, Sicsic C, et al. Inhibitory effect of carbamazepine on inflammatory mediators produced by stimulated glial cells. Neurosci Res. 2000;38:209–212.

[51] Gomez CD, Buijs RM, Sitges M. The anti-seizure drugs vinpocetine and carbamazepine, but not valproic acid, reduce inflammatory IL-1beta and TNF-alpha expression in rat hippocampus. J Neurochem. 2014;130:770–779.

[52] Wong KK, Lee R, Watkins RR, et al. Prolonged clostridium difficile infection may be associated with vitamin D deficiency. JPEN J Parenter Enteral Nutr. 2016;40:682–687.

[53] Ananthakrishnan AN, Cagan A, Gainer VS, et al. Higher plasma vitamin D is associated with reduced risk of Clostridium difficile infection in patients with inflammatory bowel diseases. Aliment Pharmacol Ther. 2014;39:1136–1142.

[54] Micic D, Rao, K, Trindade, BC, et al. Serum 25-Hydroxyvitamin D levels are not associated with adverse outcomes in clostridium difficile infection. Infect Dis Rep. 2015;7:5979.

[55] Mutai WC, Mureithi MW, Anzala O, et al. High prevalence of multidrug-resistant clostridioides difficile following extensive use of antimicrobials in hospitalized patients in Kenya. Front Cell Infect Microbiol. 2020;10:604986.

[56] Lew T, Putsathit P, Sohn KM, et al. Antimicrobial susceptibilities of Clostridium difficile Isolates from 12 Asia-Pacific Countries in 2014 and 2015. Antimicrob Agents Chemother. 2020;64. DOI:10.1128/AAC.00296-20.

[57] Harusato A, Geem D, Denning TL. Macrophage Isolation from the mouse small and large intestine. Methods Mol Biol. 2016;1422:171–180.

[58] Winston JA, Thanissery R, Montgomery SA, et al. Cefoperazone-treated mouse model of clinically-relevant Clostridium difficile strain R20291. J Vis Exp. 2016. DOI:10.3791/54850

[59] Ho J, Chan H, Liang Y, et al. Cathelicidin preserves intestinal barrier function in polymicrobial sepsis. Crit Care. 2020;24:47.

[60] Murai IH, Fernandes AL, Sales LP, et al. Effect of a single high dose of Vitamin D3 on hospital length of stay in patients with moderate to severe COVID-19. JAMA. 2021;325:1053–1060.

[61] Zuo T, Wong SH, Cheung CP, et al. Gut fungal dysbiosis correlates with reduced efficacy of fecal microbiota transplantation in Clostridium difficile infection. Nat Commun. 2018;9:3663.

[62] Reeves AE, Theriot CM, Bergin IL, et al. The interplay between microbiome dynamics and pathogen dynamics in a murine model of Clostridium difficile Infection. Gut Microbes. 2011;2:145–158.